

Kinetic Investigations of SiMn Slags From Different Mn-sources

Pyunghwa Peace Kim
Merete Tangstad

Department of Materials Science and Engineering
Norwegian University of Science and Technology (NTNU)
N-7491 Trondheim, Norway

pyung.h.kim@ntnu.no
merete.tangstad@ntnu.no

Abstract

The kinetics of MnO and SiO₂ reduction were investigated for SiMn slags by using a TGA furnace between 1773 and 1923 K (1500 and 1650 °C) under CO atmospheric pressure. The charge materials were based on Assmang ore and HC FeMn Slag. Rate models for MnO and SiO₂ reduction were considered to describe the metal-producing rates, which are shown by the following equations:

$$r_{MnO} = k_{Mn} \cdot A \cdot \left(a_{MnO} - \frac{a_{Mn} \cdot p_{CO}}{K_T} \right)$$

$$r_{SiO_2} = k_{Si} \cdot A \cdot \left(a_{SiO_2} - \frac{a_{Si} \cdot p_{CO}^2}{K_T} \right)$$

The results showed that the choice of raw materials in the charge gave considerable difference to the reduction rate of MnO and SiO₂, where the highest reduction rate was found to be from charges using HC FeMn slag. The difference in the driving forces was insignificant among the SiMn slags, and the comparison of the slag viscosities was rather similar which could not explain the different reduction rates. Instead, small amount of sulfur and initial amount of iron in the charge gave implication to the enhanced reduction rates. In addition, the considered rate models were applicable to describe the reduction of MnO and SiO₂ in SiMn slags.

KeyWords

SiMn, MnO, SiO₂, Reduction, Kinetics

32

I. Introduction

33 The production of silicomanganese (SiMn) is an important process due to its contribution to the steel
 34 producing industries. It is well known that Mn as an alloying unit enhances the strength, toughness and
 35 hardness of steel products, and both Mn and Si are excellent deoxidizers which prevent porous structures
 36 ^[1-8]. The standard SiMn alloy typically contains approximately 70 wt% Mn, 18~20 wt% Si and 10 wt% Fe
 37 ^[2].

38 While manganese thermodynamics have been studied intensively during the past two decades ^[2], kinetic
 39 information in the SiMn process is however scarce. The absence of kinetic information increases the
 40 ambiguousness of the reduction mechanisms, and it is not clear how different raw materials affect the
 41 reduction of MnO and SiO₂ in the SiMn process. The metal producing reactions in the SiMn process are
 42 described by the following reactions:



45 Previous studies have shown that both MnO and SiO₂ reduction becomes significant above 1773 K (1500
 46 °C) ^[9, 10]. The mass loss observed from a TGA furnace, which indicates MnO and SiO₂ reduction, was
 47 insignificant until 1773 K (1500 °C) but increased drastically at higher temperatures. Therefore, the present
 48 study focuses on estimating the kinetic parameters, such as activation energies and rate constants, in
 49 different SiMn slags (MnO-SiO₂-CaO-MgO-Al₂O₃) between 1773 and 1923 K (1500 and 1650 °C). The
 50 main goal is to describe the reduction rates of MnO and SiO₂ in SiMn slags from raw material Mn-sources
 51 such as Assmang ore and HC FeMn slag (High-Carbon Ferromanganese slag).

52

53

II. Theoretical Considerations

54 Previous studies have shown that the reduction rate of MnO in ferromanganese (FeMn) slags can be
 55 described by Eq. (1), which implies that the chemical reaction is the rate determining step ^[2, 11]. SiMn slags
 56 are essentially similar to FeMn slags, and the same rate expression for MnO reduction can be presumed.
 57 Assuming that SiO₂ reduction in SiMn slags is also controlled by chemical reaction, a similar rate model
 58 can be considered by Eq. (2), which was presumed and used for estimating the kinetic parameters in this
 59 work:

$$60 \quad r_{MnO} = k_{MnO} \cdot A \cdot \left(a_{MnO} - \frac{a_{Mn} \cdot p_{CO}}{K_T} \right) = k_{o,MnO} \cdot A \cdot e^{-E_{MnO}/RT} \cdot \left(a_{MnO} - \frac{a_{Mn} \cdot p_{CO}}{K_{T,MnO}} \right) \quad (1)$$

$$61 \quad r_{SiO_2} = k_{SiO_2} \cdot A \cdot \left(a_{SiO_2} - \frac{a_{Si} \cdot p_{CO}^2}{K_T} \right) = k_{o,SiO_2} \cdot A \cdot e^{-E_{SiO_2}/RT} \cdot \left(a_{SiO_2} - \frac{a_{Si} \cdot p_{CO}^2}{K_{T,SiO_2}} \right) \quad (2)$$

62 Where r (g/min) is the reduction rate, k (g/min·cm²) is the rate constant, k_o is the pre-exponential constant,
 63 A (cm²) is the reaction interface, E (kJ/mol) is the activation energy, R is the ideal gas constant, T (K) is
 64 the temperature, a_{MnO} , a_{SiO_2} are the activity of MnO and SiO₂ in the slag phase, a_{Mn} , a_{Si} are the activity of
 65 Mn and Si in the metal phase, p_{CO} is the partial pressure of CO (g) and K_T is the equilibrium constant at
 66 temperature T .

67 The rate models for MnO and SiO₂ reduction also imply that the driving force for reduction, which is the
 68 difference between actual and equilibrium activities, contribute to the reduction rates. Simplified models
 69 for activities of slag (MnO, SiO₂) and metal (Mn, Si) components in their respective melts have been

70 recently studied and were expressed as Eqs. (3 ~ 6) ^[12]. These activities were derived based on FactSage
 71 7.0 ^[13] and used to calculate the driving forces for MnO and SiO₂ reduction.

$$\begin{aligned}
 72 \quad a_{MnO} = & C_{MnO} \cdot \exp(0.0007576T - 123.7C_{MnO} + 30.14C_{SiO_2} + 47.84C_{MgO} + 49.54C_{CaO} - 47.96C_{Al_2O_3} \\
 73 & + 122.8C_{MnO}^2 - 67.78C_{SiO_2}^2 - 46.32C_{MgO}^2 - 47.68C_{CaO}^2 + 22.51C_{Al_2O_3}^2 + 78.35C_{MnO}C_{CaO} \\
 74 & + 77.56C_{MnO}C_{MgO} + 176.6C_{MnO}C_{Al_2O_3} + 101.2C_{MnO}C_{SiO_2} - 71.52C_{SiO_2}C_{CaO} - 70.58C_{SiO_2}C_{MgO} \\
 75 & + 27.35C_{SiO_2}C_{Al_2O_3} + 46C_{SiO_2}^3 - 92.97C_{CaO}C_{MgO} + 2.44C_{CaO}^3) \quad (3)
 \end{aligned}$$

$$\begin{aligned}
 76 \\
 77 \quad a_{SiO_2} = & C_{SiO_2} \cdot \exp(-0.0003408T + 113.8C_{MnO} - 22.79C_{SiO_2} - 51.63C_{MgO} - 52.44C_{CaO} + 36.3C_{Al_2O_3} \\
 78 & - 119.3C_{MnO}^2 + 42.56C_{SiO_2}^2 + 32.25C_{MgO}^2 + 30.12C_{CaO}^2 - 26.26C_{Al_2O_3}^2 - 82.725C_{MnO}C_{CaO} \\
 79 & - 82.9C_{MnO}C_{MgO} - 155.2C_{MnO}C_{Al_2O_3} - 86.98C_{MnO}C_{SiO_2} + 86.21C_{SiO_2}C_{CaO} + 86.19C_{SiO_2}C_{MgO} \\
 80 & - 23.06C_{SiO_2}C_{Al_2O_3} - 31.26C_{SiO_2}^3 + 69.45C_{CaO}C_{MgO} + 11.29C_{CaO}^3) \quad (4)
 \end{aligned}$$

$$\begin{aligned}
 81 \\
 82 \quad a_{Mn} = & C_{Mn} \cdot \exp(0.0005382T - 37.41C_{Mn} - 2.966C_{Si} - 0.6835C_{Fe} + 39.52C_{Mn}^2 - 1.453C_{Si}^2 \\
 83 & - 0.5561C_{Fe}^2 + 27.48C_{Mn}C_{Si} + 38.69C_{Mn}C_{Fe} + 0.214C_{Si}C_{Fe}) \quad (5)
 \end{aligned}$$

$$\begin{aligned}
 84 \\
 85 \quad a_{Si} = & C_{Si} \cdot \exp(0.002464T + 10.3C_{Mn} - 1.081C_{Si} + 27.52C_{Fe} - 15.49C_{Mn}^2 - 3.713C_{Si}^2 - 34.66C_{Fe}^2 \\
 86 & + 1.324C_{Mn}C_{Si} - 47.01C_{Mn}C_{Fe} - 9.127C_{Si}C_{Fe}) \quad (6)
 \end{aligned}$$

87 Where C_{MnO} , C_{SiO_2} , C_{CaO} , C_{MgO} , $C_{Al_2O_3}$ are the mass fraction of MnO, SiO₂, CaO, MgO, Al₂O₃ in the slag
 88 phase, and C_{Mn} , C_{Si} , C_{Fe} , C_C are the mass fraction of Mn, Si, Fe, C in the metal phase, respectively.

89

90

III. Experimental Procedures

91 The focus of this work was to study the reaction rates and to estimate the kinetic parameters of MnO and
 92 SiO₂ reduction in SiMn slags. The characterization and preparation of SiMn charges, the TGA furnace and
 93 the experimental conditions are described in the following sub-sections.

A. Raw materials preparation

95 Three different SiMn charges based on Assmang ore and HC FeMn slag were used in this work. The
 96 composition of raw materials and the charge compositions are shown in Tables 1 and 2, respectively. The
 97 raw materials were analyzed by SINTEF (MOLAB) ^[14], and the particle sizes were between 0.6 ~ 1.6 mm.
 98 The amount of each raw material was considered to aim at approximately 40 wt % SiO₂ and 5 wt % MnO
 99 in slag and 18 wt % Si in metal phase, which is close to the thermodynamic equilibrium at 1873 K (1600
 100 °C) ^[2]. The raw materials in each charge type were added as layers into the graphite crucibles (36 mm outer
 101 diameter, 30 mm inner diameter, 70 mm height and 61 mm deep) with the low melting materials at the top
 102 and the carbon at the bottom.

103

Table 1. Chemical compositions of raw materials

Material	MnO	MnO ₂	SiO ₂	Fe ₂ O ₃	CaO	MgO	Al ₂ O ₃	S	C	CO ₂	H ₂ O	Total [wt%]
Assmang	32.69	33.22	5.77	15.06	6.26	1.1	0.26	0.16	0.27	3.52	1.55	99.86
Quartz	0.14	-	93.85	-	0.09	0.05	1.19	-	-	-	-	95.32
HCS*	35.23	-	25.45	-	18.45	7.53	12.3	0.46	0.46	-	2.2	102.08
Coke	0.04	-	5.6	0.86	0.42	0.22	2.79	0.4	87.68	-	15.5	113.51

104 * HCS: High Carbon FeMn Slag

105

107

Table 2. Charge compositions based on Assmang ore and HC FeMn slag

Charge	Assmang	Quartz	HCS	Coke	Total [g]	C+M/A***
As**	7	1.94	-	2.2	11.14	12.22
As/HCS	4	1.69	4	2.5	12.19	2.56
HCS	-	1.46	10	3	14.46	2.08

108

** As: Assmang Ore

109

*** C+M/A: CaO+MgO/Al₂O₃

110

111

B. TGA furnace and experimental conditions

112

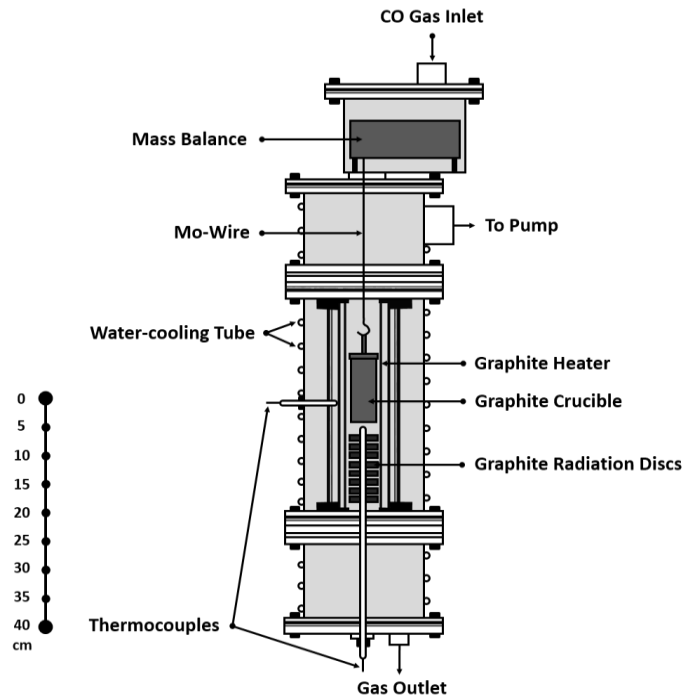
The experiments were conducted by using a TGA furnace, which is schematically shown in Figure 1. The furnace can endure temperatures up to 1973 K (1700 °C) and the maximum heating rate is up to 25 K/min. A mass balance is installed at the top and a Molybdenum (Mo)-wire was used to suspend the graphite crucible inside the furnace chamber. A B-type thermocouple was placed 1cm beneath the graphite crucible to measure the temperatures.

113

114

115

116



117

118

Fig. 1 – Schematic of the TGA furnace

119

The heating of the furnace was programed to follow a temperature schedule which is described in Figure 2. Initially, the furnace was rapidly heated up to 1473 K (1200 °C) (+25 K/min) and held for 30 minutes to secure complete degree of pre-reduction^[2]. Then, further heating (+4.5 K/min) was done and stopped at temperatures between 1773 and 1923 K (1500 and 1650 °C). This temperature profile was considered to simulate the industrial furnace process. 16 experiments for each charge type with a temperature difference of 10 K (10 °C) were conducted between 1773 and 1923 K (1500 and 1650 °C).

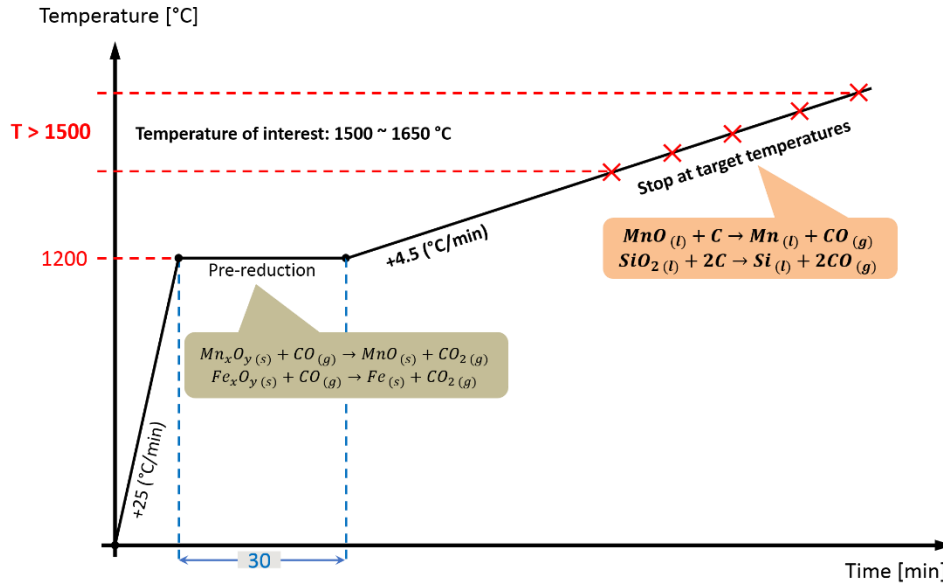
120

121

122

123

124



125

126

Fig. 2 – Temperature schedule

127 All experiments were conducted in CO atmospheric pressure (0.5 l/min CO) to simulate the industrial
 128 environment, and the mass change data were logged every 5 seconds. Lastly, charge samples were prepared
 129 by mounting epoxy to be further analyzed.

130 The charge samples were ground, polished and analyzed by an EPMA (Electron Probe Micro Analyzer):
 131 JEOL JXA-8500F. More than 5 random points in the slag phase were analyzed for each phase, and the
 132 corresponding metal compositions were calculated based on the average slag composition. As the metal
 133 analyses are more uncertain than the slag analyses, the slag analyses were used to estimate the amount of
 134 MnO and SiO₂ reduction.

135

136

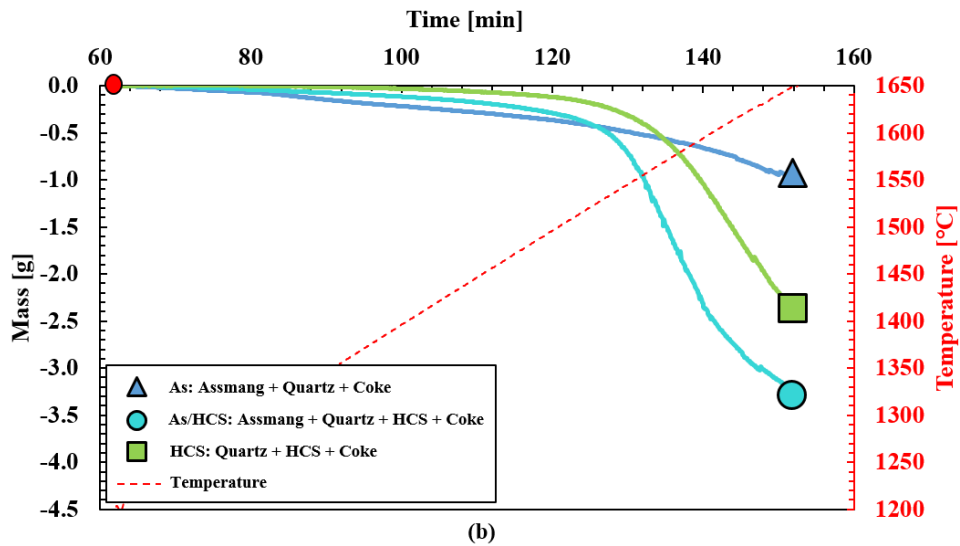
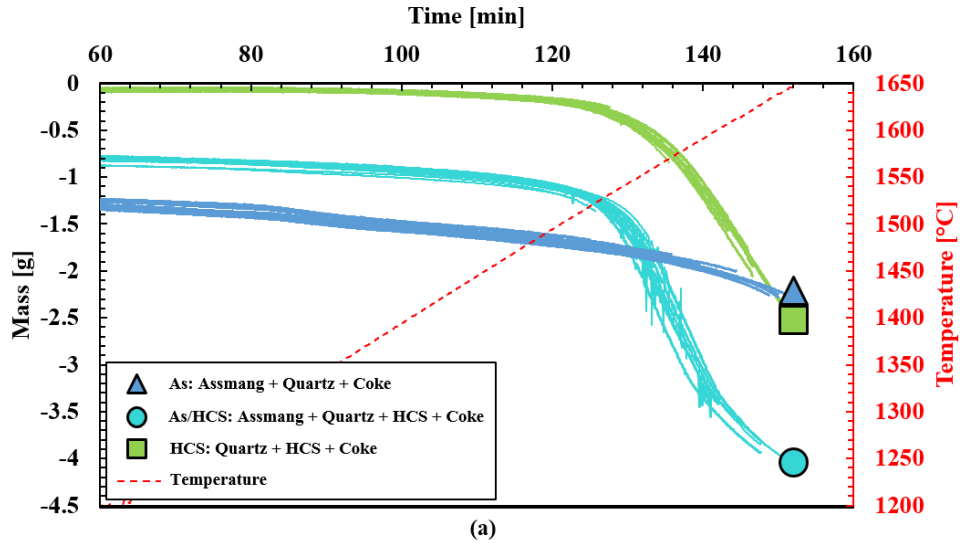
IV. Results and Discussions

137 The objective of this study was to empirically find kinetic parameters and evaluate the presumed rate
 138 models for MnO and SiO₂ reduction in SiMn slags between 1773 and 1923 K (1500 and 1650 °C). The
 139 results of the following aspects are described and discussed in sub-sections: TGA results, Slag/Metal
 140 composition, Arrhenius plots and Rate models.

141

142 A. TGA results and Slag/Metal composition

143 The main information from the TGA furnace is the mass change of the charge materials during the
 144 experimental condition. Figure 3 describes the average TGA results of 16 experiments for each charge type
 145 between 1773 to 1923 K (1200 to 1650 °C). Note that a complete degree of pre-reduction was assumed at
 146 1473 K (1200 °C) and used as a new reference point for further reduction of MnO and SiO₂.



147
 148 Fig. 3 – TGA results: 16 experiments for each charge type (a), and the average mass changes with a new
 149 reference point (red circle) at 1473 K (1200 °C) (b)

150 The mass change for all charge types below 1773 K (1500 °C) were insignificant, which indicated low
 151 degree of MnO and SiO₂ reduction. However, the mass changes increased at higher temperatures, and the
 152 reduction rates of MnO and SiO₂ seem to accelerate above 1773 K (1500 °C), especially for the two charges
 153 with HC FeMn slags, “As/HCS” and “HCS”.

154 While a drastic change in both “As/HCS” and “HCS” was observed, the same result was not seen in
 155 “As”, where no HC FeMn slag was used, even until 1923 K (1650 °C). The lower mass change of “As”
 156 indicates lower degree of MnO and SiO₂ reduction compared to “As/HCS” and “HCS”, and also resembles
 157 the mass changes previously seen in FeMn charges^[9]. The reduction of “As” seems linear and progressive
 158 between 1473 and 1873 K (1200 and 1600 °C). Nevertheless, the TGA result does not describes the
 159 reduction degrees of MnO and SiO₂ separately. To determine the reduction degrees of MnO and SiO₂,
 160 quantitative slag and metal composition is required.

161 The average chemical compositions of slag and the corresponding calculated metal with their respective
 162 activities (slag: a_{MnO} and a_{SiO_2} , metal: a_{Mn}/K_T and a_{Si}/K_T) between 1773 and 1923 K (1500 to 1650 °C) in 3
 163 different charge types are shown in Table 3. The different reduction degrees of MnO in the 3 charges were
 164 clearly observed from Table 3 between 1773 and 1923 K (1500 to 1650 °C). The MnO content in “As”
 165 drops from approximately 51 to 46 wt %, which indicated a low degree of MnO reduction. On the other
 166 hand, considerable amount of MnO reduction can be observed from “As/HCS” and “HCS”. The changes
 167 in MnO amount were approximately from 41 to 5 wt % and from 32 to 7 wt % in “As/HCS” and “HCS”,
 168 respectively. In addition, the a_{MnO} showed good accordance of the changing amount of MnO. While the
 169 decrease of a_{MnO} in “As” was insignificant, it was clear in “As/HCS” and “HCS”. For the two latter cases,
 170 the a_{MnO} was approximately 0.2 at 1773 K (1500 °C) and gradually decreased near to 0 at 1923 K (1650
 171 °C), which also indicates the higher reduction degree of MnO.

172 Table 4 describes the slag composition in absolute amount (g), where the amount of each slag and metal
 173 component were calculated assuming constant amount of unreducible oxides, CaO, MgO and Al₂O₃, for
 174 each temperature. Note that the amount of MnO and SiO₂ at 1473 K (1200 °C) was also calculated assuming
 175 complete degree of pre-reduction to use as a reference point.

176 Table 4 shows the clear change of slag (MnO, SiO₂) and metal (Mn, Si) between 1773 to 1923 K (1500
 177 to 1650 °C). The amount of MnO and SiO₂ decreases gradually with increasing temperature, and the amount
 178 of Mn and Si increases accordingly. To compare the reduction extent of MnO and SiO₂ from the initial slag
 179 composition (calculated slag composition at 1473 K), simple Eqs. (7, 8) were used to describe the reduction
 180 degrees in a scale of 0 ~ 1. Figure 4 shows the MnO and SiO₂ reduction degrees of the 3 different charges.

$$181 \quad \text{Reduction Degree}_{(\text{MnO})} = \frac{\text{Produced Mn [g]}}{\text{Initial MnO [g]}} \times \frac{70.97 [\text{g MnO/mol}]}{54.94 [\text{g Mn/mol}]} \quad (7)$$

$$182 \quad \text{Reduction Degree}_{(\text{SiO}_2)} = \frac{\text{Produced Si [g]}}{\text{Initial SiO}_2 [\text{g}]} \times \frac{60.08 [\text{g SiO}_2/\text{mol}]}{28.09 [\text{g Si/mol}]} \quad (8)$$

183

184

185 Table 3. Relative amount of slag and metal compositions with their respective activities for 3 different
 186 charges between 1773 and 1923 K (1500 and 1650 °C)

Charge-Temp.	Slag (EPMA) [wt %]								C+M/A	Metal (Calculated) [wt %]					
	MnO	SiO ₂	CaO	MgO	Al ₂ O ₃	a _{MnO}	a _{SiO₂}	Mn		Si	Fe	C	a _{Mn} /K _T	a _{Si} /K _T	
As-1500	50.6	39.1	7.6	1.2	0.5	0.152	0.285	17.2	54.6	4.3	35.9	5.2	0.0037	0.1280	
1510	49.3	40.5	7.7	1.3	0.7	0.137	0.339	13.7	55.9	2.0	35.9	6.2	0.0035	0.0378	
1520	51.3	37.9	7.2	1.3	0.5	0.171	0.237	16.0	54.4	7.4	34.0	4.2	0.0030	0.1914	
1530	50.5	38.8	7.7	1.2	0.5	0.160	0.269	16.4	55.2	5.8	34.3	4.6	0.0029	0.0994	
1540	51.4	37.4	8.4	0.7	0.7	0.181	0.218	13.3	55.0	8.8	32.6	3.5	0.0026	0.1598	
1550	50.1	38.7	8.3	0.8	0.7	0.165	0.258	12.7	56.4	7.4	32.2	4.1	0.0025	0.0915	
1560	50.8	37.9	7.5	1.4	0.5	0.177	0.229	16.3	55.8	8.7	31.7	3.8	0.0021	0.1026	
1570	49.0	39.7	7.7	1.3	0.5	0.155	0.289	16.6	57.6	6.7	31.3	4.5	0.0021	0.0504	
1580	49.4	39.0	8.6	0.7	0.8	0.165	0.261	11.7	57.5	8.1	30.6	3.9	0.0019	0.0543	
1590	50.1	38.2	8.9	0.8	0.7	0.179	0.230	13.4	57.1	9.4	30.1	3.4	0.0017	0.0587	
1600	49.1	38.7	8.9	0.7	0.9	0.173	0.243	11.1	58.3	9.7	28.6	3.5	0.0016	0.0511	
1610	48.4	38.8	9.1	0.7	0.8	0.173	0.240	12.5	59.1	10.4	27.3	3.2	0.0015	0.0479	
1620	48.7	37.7	9.4	0.7	0.9	0.193	0.198	11.0	59.2	12.3	25.8	2.7	0.0013	0.0581	
1630	46.1	40.5	8.0	1.4	0.8	0.154	0.289	11.6	60.8	9.9	25.6	3.6	0.0013	0.0311	
1640	45.7	40.1	9.3	1.4	0.8	0.162	0.263	13.3	61.1	11.3	24.3	3.3	0.0011	0.0339	
1650	48.1	37.3	7.5	1.3	0.7	0.208	0.175	12.0	59.6	13.5	24.2	2.8	0.0009	0.0443	
As/HCS-1500	40.5	35.1	12.3	3.8	5.2	0.210	0.107	3.1	50.0	10.7	36.5	2.9	0.0031	0.6101	
1510	39.8	35.4	12.2	3.5	5.8	0.204	0.111	2.7	52.7	10.6	33.8	3.0	0.0030	0.4818	
1520	39.1	36.6	12.0	3.9	5.6	0.184	0.135	2.9	54.5	5.2	35.6	4.7	0.0032	0.1010	
1530	39.1	35.7	12.1	3.7	4.9	0.200	0.113	3.3	54.6	10.5	31.8	3.1	0.0026	0.2934	
1540	38.3	36.8	12.2	3.9	5.0	0.182	0.135	3.2	56.8	6.4	32.4	4.4	0.0028	0.0904	
1550	34.1	39.0	13.2	3.7	6.3	0.143	0.168	2.7	64.8	6.5	24.1	4.6	0.0029	0.0734	
1560	29.5	40.4	14.4	4.0	6.7	0.115	0.182	2.7	68.4	8.9	18.7	3.9	0.0027	0.1021	
1570	24.0	41.8	16.2	4.3	8.0	0.087	0.187	2.6	70.2	11.1	15.3	3.4	0.0024	0.1244	
1580	19.7	44.1	18.3	5.2	8.8	0.062	0.227	2.7	72.0	10.3	14.1	3.7	0.0023	0.0838	
1590	17.2	44.2	19.2	5.2	9.2	0.054	0.212	2.7	71.8	11.6	13.2	3.4	0.0020	0.0882	
1600	12.7	43.8	21.6	6.2	10.4	0.039	0.174	2.7	71.3	13.9	12.0	2.9	0.0016	0.1094	
1610	12.3	45.4	21.2	6.0	10.7	0.035	0.213	2.6	72.2	12.4	12.1	3.2	0.0016	0.0682	
1620	10.9	44.6	22.5	6.4	11.5	0.032	0.183	2.5	71.6	13.7	11.7	3.0	0.0014	0.0710	
1630	6.8	45.5	24.2	6.7	12.4	0.018	0.181	2.5	71.8	14.1	11.1	2.9	0.0013	0.0637	
1640	6.8	44.0	24.9	7.2	12.8	0.020	0.147	2.5	71.0	15.2	11.0	2.8	0.0011	0.0651	
1650	4.9	43.9	26.5	7.1	13.8	0.014	0.136	2.4	70.9	15.7	10.7	2.8	0.0010	0.0591	
HCS-1500	31.7	34.5	15.4	4.9	9.4	0.171	0.076	2.2	27.3	30.1	36.2	6.4	0.0005	-	
1510	31.7	34.2	15.8	5.0	9.7	0.176	0.072	2.2	29.7	32.4	27.2	10.7	0.0002	-	
1520	31.5	34.1	15.9	5.1	9.7	0.178	0.069	2.2	35.5	32.1	22.2	10.2	0.0002	-	
1530	30.8	33.8	15.8	5.2	10.0	0.179	0.064	2.1	43.8	31.5	15.0	9.6	0.0001	-	
1540	31.7	34.4	15.8	5.5	9.2	0.177	0.074	2.3	28.6	30.7	33.2	7.6	0.0002	-	
1550	30.6	35.8	16.1	5.6	9.5	0.155	0.092	2.3	58.6	0.1	34.5	6.9	0.0027	-	
1560	30.0	35.7	16.3	5.8	9.7	0.154	0.090	2.3	63.9	8.8	23.5	3.9	0.0025	0.1012	
1570	27.6	35.6	16.9	5.8	10.0	0.143	0.080	2.3	68.5	18.9	10.1	2.5	0.0013	0.5175	
1580	24.1	38.8	17.3	5.5	11.3	0.098	0.124	2.0	82.1	3.4	8.2	6.3	0.0028	0.0126	
1590	23.7	38.4	17.5	5.8	11.4	0.100	0.116	2.1	80.5	7.0	7.6	5.0	0.0025	0.0302	
1600	21.2	38.8	18.5	6.2	11.5	0.086	0.114	2.2	79.9	10.4	5.9	3.9	0.0021	0.0507	
1610	17.1	40.1	19.4	6.3	12.9	0.061	0.124	2.0	80.8	10.8	4.6	3.8	0.0019	0.0444	
1620	14.3	40.8	21.3	6.8	13.3	0.047	0.127	2.1	80.8	11.6	4.0	3.7	0.0017	0.0423	
1630	11.6	41.5	22.9	7.1	13.9	0.035	0.130	2.2	80.8	12.1	3.6	3.6	0.0016	0.0385	
1640	9.2	40.2	23.6	7.8	15.3	0.028	0.097	2.0	77.7	16.4	3.2	2.9	0.0010	0.0694	
1650	7.1	40.2	25.5	7.8	15.9	0.021	0.092	2.1	77.3	17.0	3.0	2.8	0.0009	0.0657	

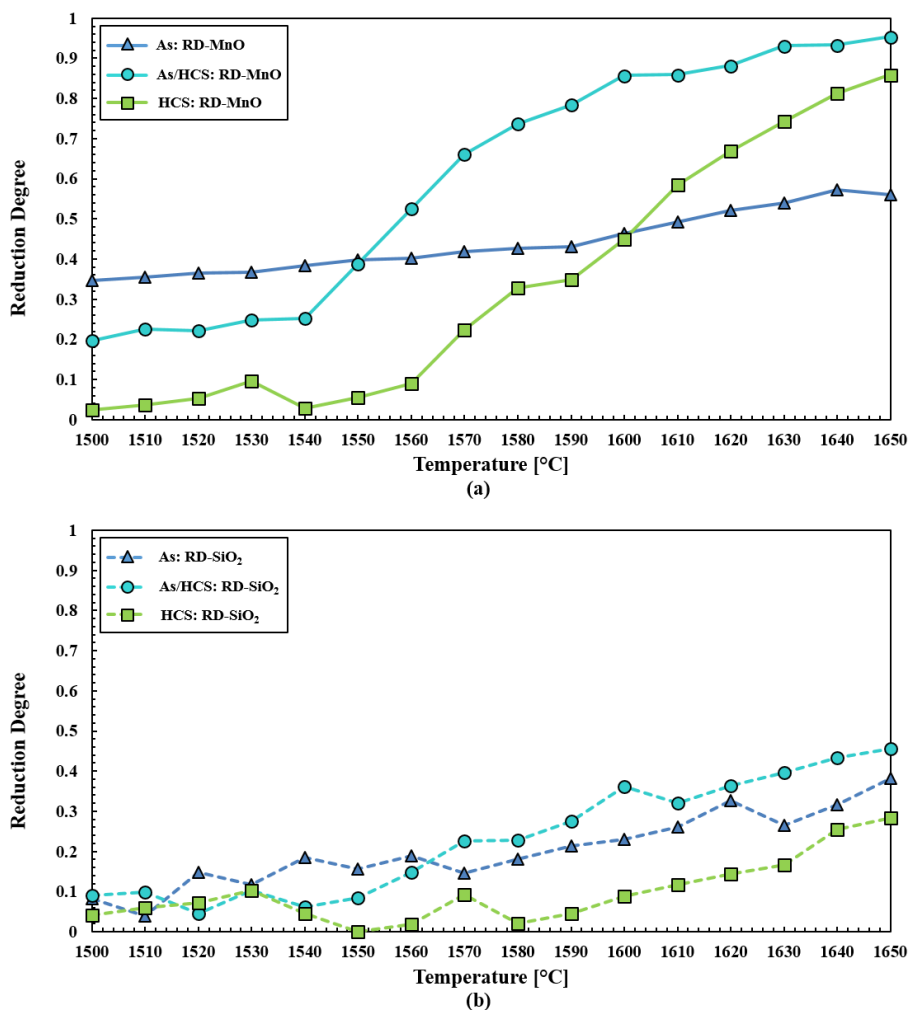
187

188
189

Table 4. Calculated absolute amount of slag and metal for 3 different charges at 1473 K (1200 °C) and between 1773 and 1923 K (1500 and 1650 °C)

Charge-Temp.	Slag [g]					Total	Metal [g]	
	MnO	SiO ₂	CaO	MgO	Al ₂ O ₃		Mn	Si
As-1200	4.2	2.3				7.1	-	-
As-1500	2.8	2.1				5.4	1.12	0.09
1510	2.7	2.2				5.5	1.15	0.04
1520	2.7	2.0				5.2	1.18	0.16
1530	2.7	2.1				5.3	1.19	0.13
1540	2.6	1.9				5.0	1.25	0.20
1550	2.5	2.0				5.0	1.30	0.17
1560	2.5	1.9				5.0	1.31	0.20
1570	2.4	2.0	0.44	0.08	0.04	5.0	1.36	0.16
1580	2.4	1.9				4.9	1.39	0.20
1590	2.4	1.8				4.8	1.40	0.23
1600	2.3	1.8				4.6	1.50	0.25
1610	2.1	1.7				4.4	1.60	0.28
1620	2.0	1.6				4.1	1.70	0.35
1630	1.9	1.7				4.2	1.76	0.29
1640	1.8	1.6				4.0	1.86	0.34
1650	1.9	1.4				3.8	1.82	0.41
As/HCS-1200	3.8	2.9				8.5	-	-
As/HCS-1500	3.0	2.6				7.5	0.58	0.12
1510	2.9	2.6				7.4	0.66	0.13
1520	3.0	2.8				7.6	0.65	0.06
1530	2.9	2.6				7.3	0.73	0.14
1540	2.8	2.7				7.4	0.74	0.08
1550	2.3	2.7				6.8	1.14	0.11
1560	1.8	2.5				6.1	1.54	0.20
1570	1.3	2.2	0.98	0.34	0.52	5.4	1.94	0.31
1580	1.0	2.2				5.1	2.16	0.31
1590	0.8	2.1				4.8	2.30	0.37
1600	0.5	1.9				4.2	2.52	0.49
1610	0.5	2.0				4.3	2.52	0.43
1620	0.5	1.8				4.1	2.59	0.49
1630	0.3	1.8				3.9	2.73	0.54
1640	0.3	1.6				3.7	2.74	0.59
1650	0.2	1.6				3.6	2.80	0.62
HCS-1200	3.7	4.0				11.5	-	-
HCS-1500	3.6	3.9				11.2	0.07	0.08
1510	3.5	3.8				11.1	0.10	0.11
1520	3.5	3.7				11.0	0.15	0.13
1530	3.3	3.6				10.7	0.27	0.20
1540	3.6	3.9				11.2	0.08	0.09
1550	3.5	4.0				11.3	0.16	0.00
1560	3.3	4.0				11.1	0.25	0.03
1570	2.8	3.7	1.82	0.74	1.23	10.3	0.63	0.17
1580	2.5	4.0				10.2	0.93	0.04
1590	2.4	3.9				10.0	0.99	0.09
1600	2.0	3.7				9.5	1.27	0.16
1610	1.5	3.6				8.9	1.65	0.22
1620	1.2	3.5				8.5	1.89	0.27
1630	0.9	3.4				8.1	2.10	0.31
1640	0.7	3.0				7.5	2.30	0.48
1650	0.5	3.0				7.2	2.43	0.53

190 The MnO and SiO₂ reduction degrees of 3 different charges are clearly described in Figure 4. The solid
 191 lines represents the reduction degree of MnO and the dotted line the reduction degree of SiO₂. “As/HCS”
 192 showed the highest reduction of MnO and SiO₂ compared to its initial amount at 1473 K (1200 °C). On the
 193 other hand, the reduction of MnO and SiO₂ in “As” was both relatively slower and lower than “As/HCS”.



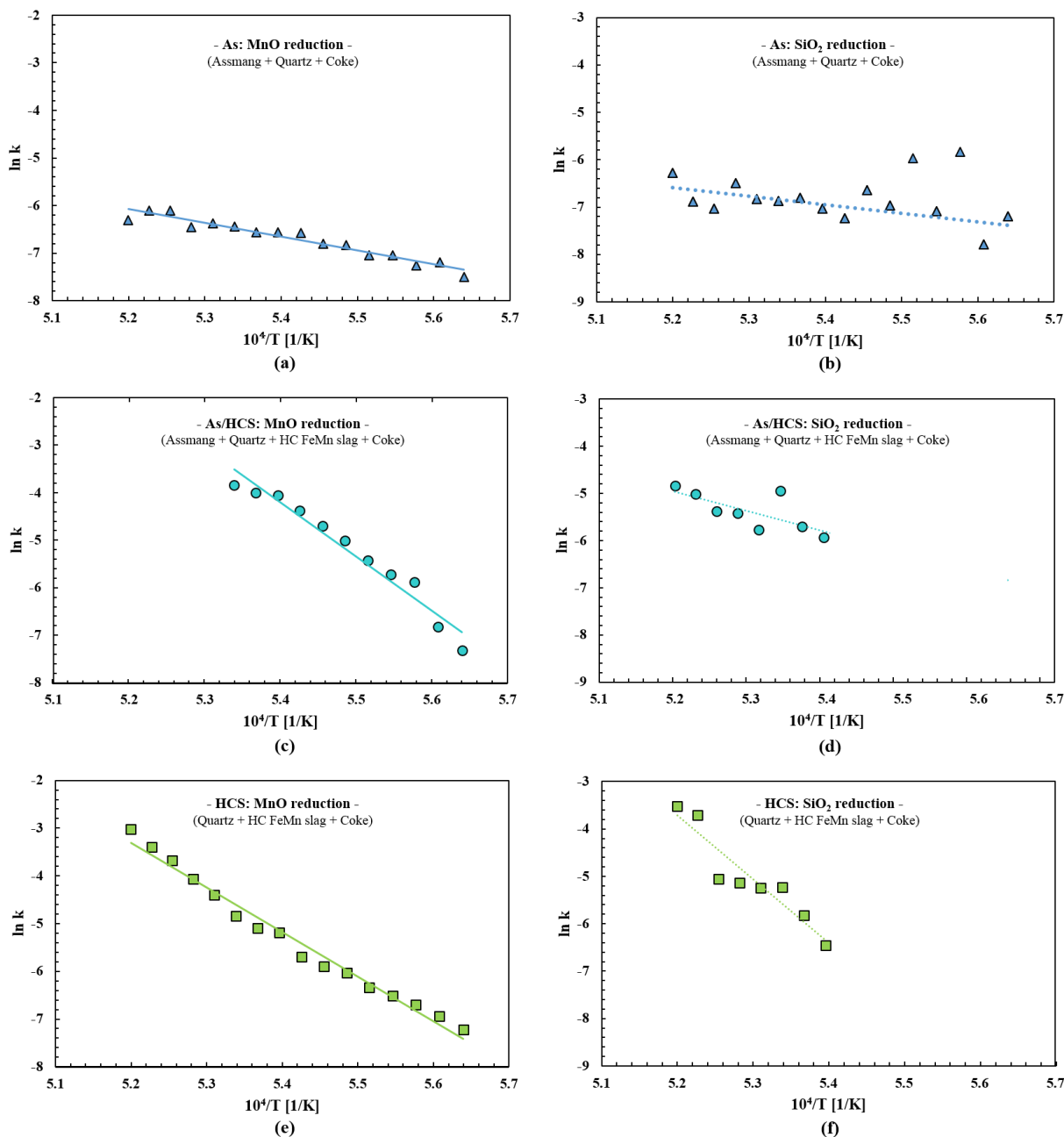
194
 195 Fig. 4 – The reduction degrees of MnO (a) and SiO₂ (b) for 3 different charge between 1773 and 1923 K
 196 (1500 and 1650 °C)

197 In addition, the a_{MnO} at 1773 K (1500 °C) was the highest in “As/HCS” and lowest in “As”, which gives
 198 implications of the different reduction degree of MnO. However, the a_{MnO} difference of the 3 different
 199 charges were not significant and thus the difference in the driving force is also assumed to be low. This
 200 implies that the rate constants should be a factor which is more comparable between the different reduction
 201 rates.

202

203 B. Arrhenius plots and Rate models

204 The Arrhenius plots for MnO and SiO₂ reduction of the 3 charges have been estimated based on the rates
 205 obtained by the TGA results and EPMA analyses. Figure 5 describes the Arrhenius plots of MnO and SiO₂
 206 reduction of the 3 charges. In addition, Table 5 summarizes the activation energies and pre-exponential
 207 constants estimated of the 3 different slags between 1773 to 1923 K (1500 and 1650 °C).



208 Fig. 5 – Arrhenius plots of MnO reduction (a, c, e) and SiO₂ reduction (b, d, f) between 1773 to 1923 K
 209 (1500 and 1650 °C)
 210
 211

212 Table 5. Summary of the activation energies and pre-exponential constants of the 3 different charges
 213 between 1773 and 1923 K (1500 and 1650 °C)

Charge	<u>MnO Reduction</u>	
	Ea [kJ/mol]	ko [g/min · cm ²]
As	~ 250	9.66 × 10 ³
As/HCS	~ 920	1.62 × 10 ²⁴
HCS	~ 780	5.87 × 10 ¹⁹
Charge	<u>SiO₂ Reduction</u>	
	Ea [kJ/mol]	ko [g/min · cm ²]
As	~ 160	3.04 × 10 ⁰
As/HCS	~ 870	5.92 × 10 ²¹
HCS	~ 1130	6.61 × 10 ²⁸

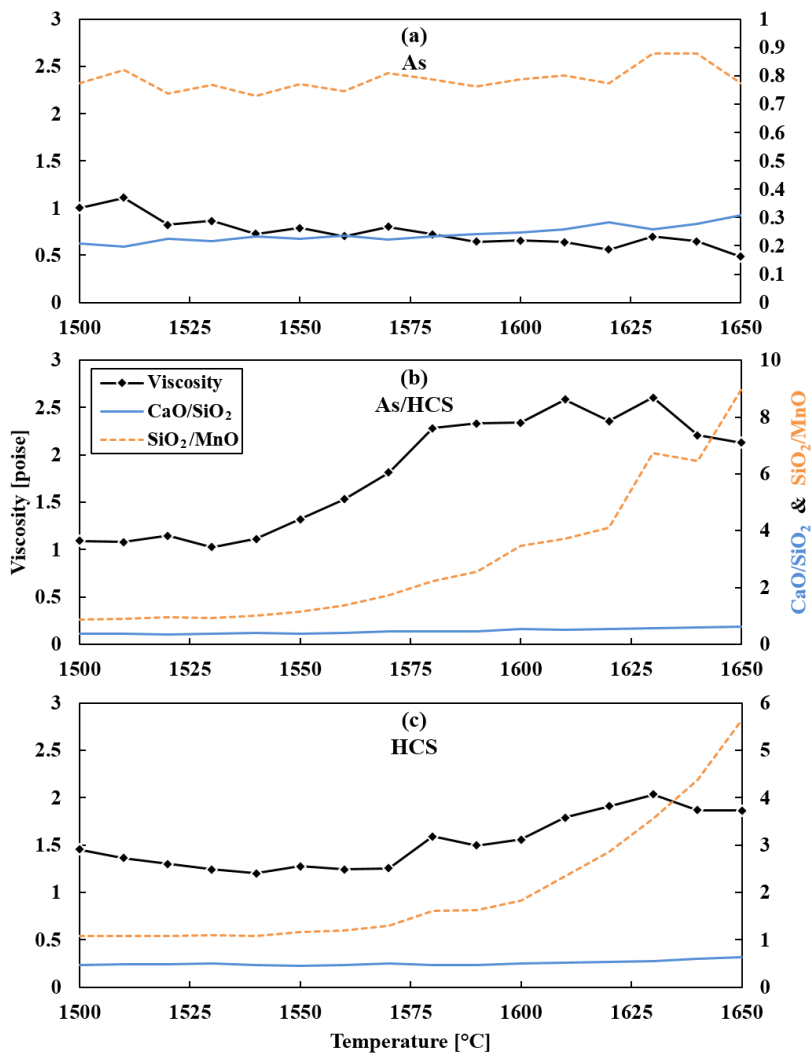
214
 215 For both MnO and SiO₂ reduction, the estimated activation energies of “As/HCS” and “HCS” were high,
 216 while this was not the case for “As”. The difference in activation energies implies that the choice of raw
 217 material for the charge can have significant impact regarding kinetics. Comparing “As” with “As/HCS”
 218 and “HCS”, it seems that HC FeMn Slag as raw material in the charge is necessary to obtain significant
 219 reduction of MnO and SiO₂. In addition, the considerably lower temperature dependency and rate constant
 220 of “As” compared to “As/HCS” and “HCS” also implies that MnO and SiO₂ reduction is hindered by kinetic
 221 factors such as viscosity and amount of trace elements.

222 The viscosities of the 3 charges between 1773 to 1923 K (1500 to 1650 °C), which were obtained by
 223 using FactSage 7.0 [13], are described in Figure 6. The increasing viscosities despite of increasing
 224 temperature in “As/HCS” and “HCS” indicates changing slag composition due to MnO reduction. On the
 225 other hand, the viscosity does not seem to explain the lower reduction degree in “As”, which shows the
 226 lowest viscosity compared to the other cases. The C+M/A ratio of “As” from Table 3 was around 12.5,
 227 which is considerably higher than “As/HCS” and “HCS”. This implies that other kinetic factors are
 228 prevalent regarding the reduction rate rather than the slag viscosity.

229 The initial amount of sulfur in slag at 1473 K (1200 °C) of the 3 different charges are shown in Table 6.
 230 Sulfur is known to behave as a strong surface-active specie for most metals [15], and the initial amount of
 231 sulfur in the charges seems to give the explanation of the different reduction rates observed. “As”, which
 232 was the lowest reduction rate, had the least amount of sulfur among the charges. The sulfur content was
 233 about twice in “As/HCS” and more in “HCS”. This implies that the amount of sulfur affects the kinetics
 234 more than the slag viscosity. This is in an accordance with recent observations where the initial sulfur
 235 content in the charge strongly affected the reduction rates of MnO and SiO₂ [10, 16].

236 The rate constants are also compared with the different amount of initial sulfur in Figure 7. There seems
 237 to be an optimal amount of sulfur regarding reduction rate. “HCS” had more sulfur content than “As/HCS”
 238 but the reduction rate was slower. Similar results were observed from a recent study using synthetic raw
 239 materials [17]. However, it is not clear whether the sulfur content gave the relatively slower reduction rate in
 240 “HCS” than “As/HCS”. The Mn-source for “HCS” was only HC FeMn slag, which lacks iron, and previous
 241 studies have shown that initial amount of iron leads to MnO reduction by dissolved carbon in the metal [18].

242 It can be a combined effect of sulfur and initial iron in the case of “As/HCS”, but further experiments are
 243 required to see which contribution is more.



244
 245 Fig. 6 – Viscosities of “As” (a), “As/HCS” (b) and “HCS” (c) compared with CaO/SiO₂ and SiO₂/MnO
 246 ratio between 1773 to 1923 K (1500 and 1650 °C)

247
 248 Table 6. Initial sulfur content of different charge types (wt % S in coke not included)

Charge type	Slag Composition at 1200 °C [wt %]					S
	MnO	SiO ₂	CaO	MgO	Al ₂ O ₃	
As	59.33	32.74	6.23	1.11	0.60	0.16
As/HCS	44.45	34.03	11.48	4.00	6.04	0.29
HCS	32.84	34.15	15.84	6.47	10.71	0.39

249

250

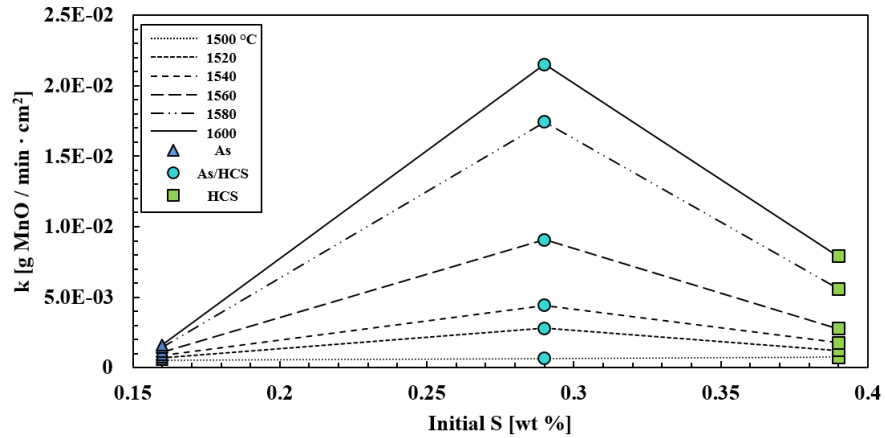
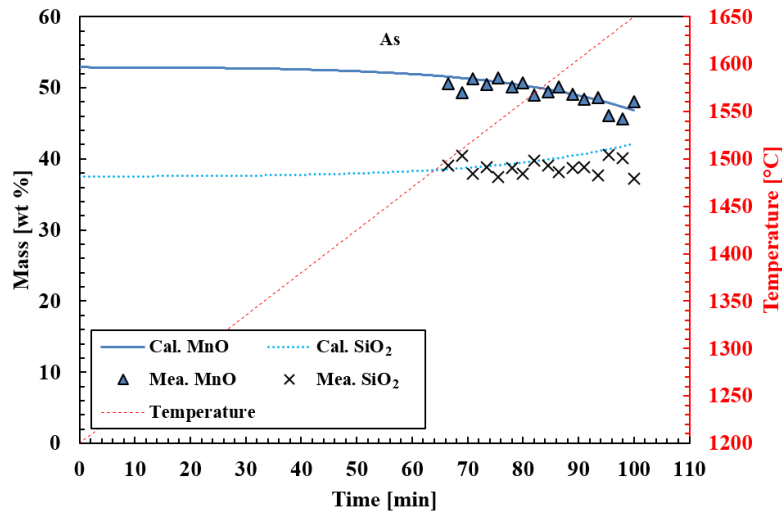


Fig. 7 – Rate constants compare with initial sulfur amount at different temperatures

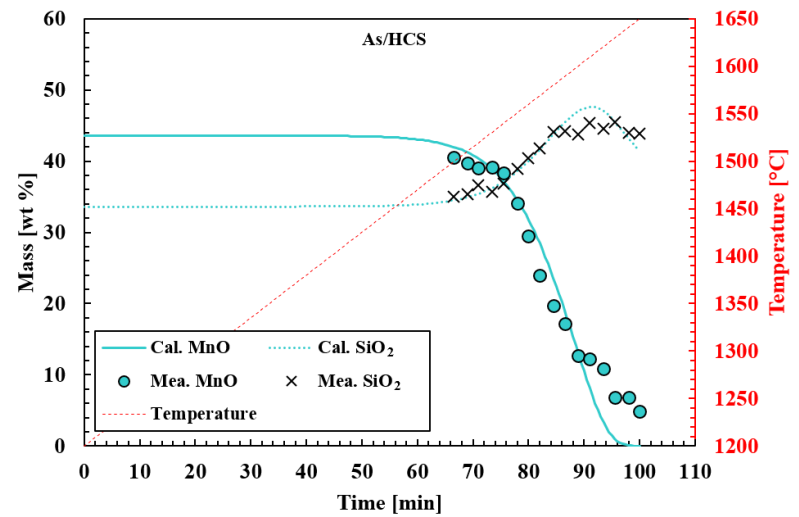
251
252

253 Based on the parameters estimated on Table 4, the reduction rates of MnO and SiO₂ in SiMn slags can
 254 be described by using the rate models, Eqs. (1, 2). The comparisons between the rate models and
 255 experimentally measured slag components (MnO and SiO₂) are shown in Figure 8. Note that the parameters
 256 which describes the best fit for the 3 charges were applied to the rate models (approximately 2 % error in
 257 the raw material analyses).

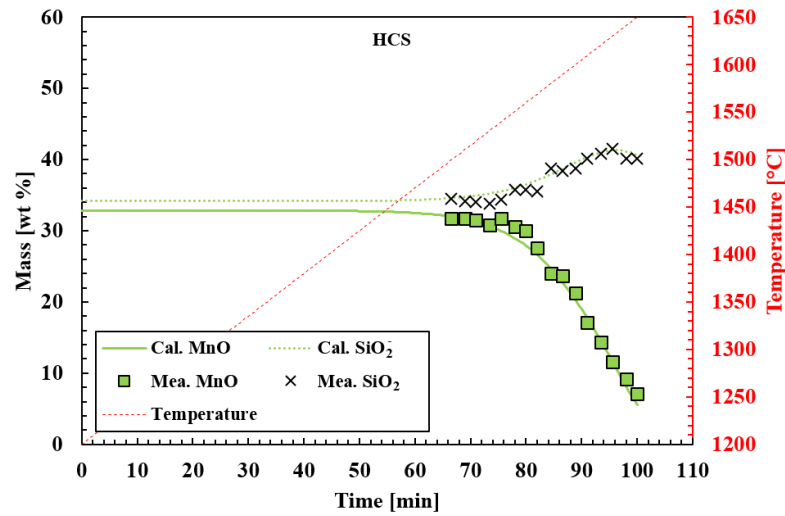
258 The comparison shows that the presumed rate models, which were based on FeMn slags in this study,
 259 are fairly applicable as well as in SiMn slags. The solid and dotted lines, which describe the relative amount
 260 of MnO and SiO₂ from the rate models, showed good match with the measured amount between 1773 to
 261 1923 K (1500 and 1650 °C). Regardless of the reduction extent, the rate models were able to describe the
 262 reduction of MnO and SiO₂ in different SiMn slags



(a)



(b)



(c)

Fig. 8 – The MnO and SiO₂ reduction obtained by using the rate models (solid and dotted lines) and the experimentally measured (symbols) for charges “As” (a), “As/HCS” (b) and “HCS” (c) between 1773 to 1923 K (1500 and 1650 °C)

V. Conclusion

The focus of this study was to estimate the kinetic parameters and evaluate the presumed rate models for MnO and SiO₂ reduction in SiMn slags. TGA results showed that most of the MnO and SiO₂ reduction starts to occur above 1773 K (1500 °C), and the charge “As/HCS” (Assmang + Quartz + HC FeMn Slag + Coke) had the fastest and highest reduction. On the other hand, “As” (Assmang + Quartz + Coke) showed the slowest and lowest reduction even up to 1923 K (1650 °C). The small difference of a_{MnO} among different slags in this case does not necessary explains the different reduction rates.

However, significant difference in kinetic parameters were estimated between “As” with “As/HCS” and “HCS” (High-carbon slag + Quartz + Coke), which implied influence from viscosity and amount of trace elements regarding the reduction rate. Comparison of viscosity showed that the different reduction rates were more affected by the small amounts of sulfur rather than the slag basicity. The effect of sulfur increasing the reduction rate was observed but further experiments are required to isolate both effects from sulfur and initial amount of iron. The presumed rate models were able to describe the reduction of MnO and SiO₂ for the different SiMn slags.

Acknowledgments

This publication has been partly funded by the SFI Metal Production, (Centre for Research-based Innovation, 237738). The authors gratefully acknowledge the financial support from the Research Council of Norway and the partners of the SFI Metal Production.

References

1. International Manganese Institute (2014), www.manganese.org. Accessed Sept 2015
2. S. E. Olsen, M. Tangstad and T. Lindstad: *Production of Manganese Ferroalloys*, Tapir Academic Press, Trondheim (Norway) 2007, pp. 15-18, 73-110, 123-126, 144-149.
3. Y. Tomota, M. Strum and J. Morris Jr.: *Metall. Trans., A*, 1987, vol. 18A, pp. 1073-1081.
4. D. K. Subramanyam, A. E. Swansiger and H. S. Avery: *Austenitic Manganese Steels in Properties and Selection: Irons, Steels and High-Performance Alloys*, 10th ed., ASM International, Ohio, OH, 1990, pp. 822-840.
5. G. F. Deev, V. V. Popovich and V. N. Palash: *Materials Science*, 1982, vol. 18, No. 3, pp. 109-112.
6. J. R. Cain: *Technological Papers of The Bureau of Standards No. 261* (Department of Commerce, USA), Jul. 30, 1924, pp. 327-335.
7. S. I. Gubenko and A. M. Galkin: *Metal Science & Heat Treatment*, Oct. 1984, vol. 26 Issue 10, pp. 732-737.
8. O. Grong, T. A. Siewert, G. P. Martins and D. L. Olson: *Metall. Trans. A*, 1986, vol. 17A, pp. 1797-1807.
9. P. Kim, J. Holtan, M. Tangstand: *Advanced in Molten Slags, Fluxes and Salts: Proceeding of The 10th International Conference on Molten Slags, Fluxes and Salts (MOLTEN 16)*, May 2016, pp. 1285-1292.
10. P. Kim, T. Larren, M. Tangstad and R. Kawamoto: *The Minerals, Metals & Materials Society 2017: Applications of Process Engineering Principles in Materials Processing, Energy and Environmental Technologies*, 2017, pp. 475-483.

11. O. Ostrovski, S. E. Olsen, M. Tangstad, M. Yastreboff: *Can. Metall. Q.*, 2002, vol. 41, No. 3, pp. 309-318.
12. H. Olsen: *A Theoretical Study on The Reaction Rates in The SiMn Production Process (Master's Thesis)*, Department of Materials Science and Engineering (DMSE), Norwegian University of Science and Technology (NTNU), Trondheim (Norway), 2016.
13. FactSage 7.0 (CRCT: Canada, GTT: Germany, www.factsage.com). Accessed Sept 2015.
14. SINTEF MOLAB (2017), www.sintefmolab.no. Accessed Sept 2015.
15. S. Stølen and T. Grande: *Chemical Thermodynamics of Materials*, Wiley, West Sussex, UK, 2004, pp. 186-190.
16. T. Larrsen: Report: TMT 4500 Materials Technology Specialization Project, Department of Materials Science and Engineering (DMSE), Norwegian University of Science and Technology (NTNU), Trondheim (Norway), 2016.
17. R. Kawamoto: Report: TMT 4500 Materials Technology Specialization Project, Department of Materials Science and Engineering (DMSE), Norwegian University of Science and Technology (NTNU), Trondheim (Norway), 2016.
18. J. Safarian and M. Tangstad: 12th International Ferroalloy Congress (INFACON), 2010, pp. 327-338.